



HAL
open science

Robust analysis of design in vibration of turbomachines

M. Mbaye, Christian Soize, J.-P. Ousty, Evangéline Capiiez-Lernout

► **To cite this version:**

M. Mbaye, Christian Soize, J.-P. Ousty, Evangéline Capiiez-Lernout. Robust analysis of design in vibration of turbomachines. 54th ASME Turbo Expo 2009, ASME, Jun 2009, Orlando, FL, United States. pp.387-396. hal-00684506

HAL Id: hal-00684506

<https://hal.science/hal-00684506>

Submitted on 2 Apr 2012

HAL is a multi-disciplinary open access archive for the deposit and dissemination of scientific research documents, whether they are published or not. The documents may come from teaching and research institutions in France or abroad, or from public or private research centers.

L'archive ouverte pluridisciplinaire **HAL**, est destinée au dépôt et à la diffusion de documents scientifiques de niveau recherche, publiés ou non, émanant des établissements d'enseignement et de recherche français ou étrangers, des laboratoires publics ou privés.

GT2009-59651

ROBUST ANALYSIS OF DESIGN IN VIBRATION OF TURBOMACHINES

Moustapha Mbaye *, **Christian Soize**
Laboratoire de Modélisation et Simulation
Multi Echelle, MSME FRE3160 CNRS
Université Paris-Est, 5 bd Descartes
77454 Marne-la-Vallée, France
moustapha.mbaye@univ-paris-est.fr
christian.soize@univ-paris-est.fr

Jean-Philippe Ousty
Turbomeca
Site de Bordes
64511 Bordes Cedex
jean-philippe.ousty@turbomeca.fr

Evangeline Capiez-Lernout
Laboratoire de Modélisation et Simulation
Multi Echelle, MSME FRE3160 CNRS
Université Paris-Est, 5 bd Descartes
77454 Marne-la-Vallée, France
evangeline.capiezlernout@univ-paris-est.fr

ABSTRACT

In the context of turbomachinery design, a small variation in the blade characteristics due to manufacturing tolerances can affect the structural symmetry creating mistuning which increases the forced response. However, it is possible to detune the mistuned system in order to reduce the forced response amplification. The main technologic solutions to introduce detuning are based on modifying blade material properties, the interface between blade and disk, or the blade shape. This paper presents a sensitivity analysis of mistuning for a given detuning in unsteady aeroelasticity. Detuning is performed by modifying blade shapes. The different kinds of blades obtained by those modifications are then distributed on the disk circumference. A new reduced-order model of the detuned disk is constructed using the cyclic modes of the different sectors which can be obtained from a usual cyclic symmetry modal analysis. Finally a stochastic analysis using a non-parametric probabilistic method to take model and system parameters uncertainties into account in the computational model is performed.

INTRODUCTION

Small variations in the blade characteristics of cyclic structures due to manufacturing tolerances affect the structural cyclic symmetry creating mistuning which increases the forced response amplitudes (e.g. see [1–3]). However, it is possible (e.g. see [4–8]) to intentionally detune the mistuned system in order to

reduce the forced response amplification. The main technologic solutions to introduce detuning are based on modifying blade material properties, the interface between blade and disk, or the blade shape by introducing several types of blades with different geometries corresponding to finite geometric perturbations of the nominal blades. In the present paper, it is assumed that detuning is performed by modifying blade shapes and the disk is not mistuned.

Vibration analysis of cyclic structures is usually performed using their cyclic symmetry and formulated for one sector from which the dynamics of the structure is obtained. This is no longer the case for mistuned structures which need a full structure formulation. To reduce numerical computational costs while solving the mistuning problem on finite element meshes of realistic bladed disks, many reduced-order methods have been introduced. In general, reduced-order models are obtained by substructuring a bladed disk into disk and blade components, as this allows for easy implementation of blade mistuning. However, a different approach [9] has been proposed by Yang and Griffin, in which the tuned system cyclic modes are used without substructuring to generate a reduced-order model. This technic is very efficient in the case of cyclic structures with material properties perturbations but do not solve the case of finite geometric perturbations. In fact, in the latter case, the tuned bladed disk sector cyclic modes are computed on a finite element mesh related to the nominal geometry and the finite mass and stiffness matrices relative to the finite geometric perturbations of certain blades are constructed with another finite element mesh which

*Adress all correspondance to this author.

is not compatible with the nominal finite element mesh. Consequently, these non compatible finite element meshes induce a difficulty for constructing the projection of the finite perturbation mass and stiffness matrices using the tuned bladed disk sector cyclic modes. That is why in [9], proportional mistuning by perturbing the Young moduli of individual blades is only simulated. To solve the problem of geometric mistuning, researchers have developed different reduced-order models among which, a simple model known as the Fundamental Mistuning Model (FMM) that reduces the set of nominal modes to a single modal family [10, 11]. Nevertheless, its application field is limited to a modal family with nearly equal frequency. Another method is the Static Mode Condensation (SMC) proposed in [12], in which the mistuned system is represented by the full tuned system and by virtual mistuning components, with convergence acceleration performed by static mode condensation. But this method needs a large amount of calculation.

In this paper, for solving the problem of detuning with geometric modification, it is assumed that a commercial software (black box) is used to compute the cyclic modes and mass and stiffness matrices of the different bladed disk sector types in independent calculations. In this particular context, we propose here a new method introduced in [13] which uses the cyclic modes of the different bladed disk sectors and which consist on reducing each sector mass and stiffness matrices by its own modes. Linear constraints are then applied on common boundaries between sectors to make the displacement field admissible.

The random nature of blade mistuning due to manufacturing tolerances and dispersion of materials has been a motivation to construct a probability model of random uncertainties to solve the stochastic forced response and to perform statistical analysis in order to predict the effects of mistuning. In this context we use a non parametric probabilistic approach which is one of the most complete probabilistic approaches by the way it takes data and model uncertainties into account, while classical parametric approaches do not allow model uncertainties to be considered. This nonparametric probability model is directly constructed using the mean reduced matrix model, and the entropy maximization principle with the available information.

CONSTRUCTION OF THE MEAN REDUCED MODEL

To construct the reduced model, we propose a new reduced-order method which is an extension of the approach proposed by Yang and Griffin in [9], and takes into account geometric modifications. Instead of projecting perturbed mass and stiffness matrices on a basis of tuned cyclic modes, our idea is to project each mass and stiffness matrix of a sector on a basis of its own cyclic modes, and to assemble the whole bladed disk reduced model by insuring the displacement field continuity between all adjacent sectors.

Dynamic equation of the detuned system

Let us consider the finite element model of a detuned structure with N blades, with detuning resulting on finite geometric perturbations of some blades, in the frequency band \mathbb{B} defined by $\mathbb{B} = [\omega_{min}, \omega_{max}]$, $0 < \omega_{min} < \omega_{max}$. Then, the dynamic equation of the detuned bladed disk can be written in the frequency band \mathbb{B}

$$(-\omega^2 [\underline{M}] + i\omega [\underline{D}] + [\underline{K}])\underline{u}(\omega) = \underline{f}_{exc}(\omega) + \underline{f}_{aero}(\omega, \underline{u}(\omega)), \quad (1)$$

where \underline{f}_{exc} denotes the vector of unsteady loads on blades due to an aerodynamic excitation source and \underline{f}_{aero} denotes the vector of unsteady coupling loads on blades due to blades motions, \underline{u} is the displacement field of the complete detuned structure, matrices $[\underline{M}]$, $[\underline{D}]$, $[\underline{K}]$ represent real mass, damping and stiffness matrices, and $i^2 = -1$. n_{dof} is the size of vectors \underline{u} which is different to the entire bladed disk degrees-of-freedom number of the whole structure, because there are some redundant degrees-of-freedom in \underline{u} due to the fact we consider each sector with its inner and boundaries degrees of freedom. By introducing the dynamic stiffness matrix

$$[\underline{E}(\omega)] = -\omega^2 [\underline{M}] + i\omega [\underline{D}] + [\underline{K}], \quad (2)$$

the dynamic equation of the detuned bladed disk becomes

$$[\underline{E}(\omega)]\underline{u}(\omega) = \underline{f}_{exc}(\omega) + \underline{f}_{aero}(\omega, \underline{u}(\omega)). \quad (3)$$

Reduced-order model of the mistuned bladed disk

Let us reduce the model by using a modal basis $[\Psi]$ of real modes obtained in the global cyclic coordinates system. These modes are obtained by performing a discrete Fourier transform of the displacement field.

Projection basis: The projection basis is written

$$[\Psi] = \begin{pmatrix} \psi_1^{\Omega_0} & \dots & \psi_{\alpha^*}^{\Omega_0} \\ \vdots & \ddots & \vdots \\ \psi_1^{\Omega_{N-1}} & \dots & \psi_{\alpha^*}^{\Omega_{N-1}} \end{pmatrix}, \quad (4)$$

where α^* is the number of modes selected, N is the number of blades and Ω represent a sector domain. In this context, $\psi_{\alpha^*}^{\Omega_p}$ is the real mode number α associated to the sector p . This real mode is obtained by using the corresponding complex cyclic mode $\hat{\phi}_{\beta,n} = \hat{\phi}'_{\beta,n} + i\hat{\phi}''_{\beta,n}$, $i^2 = -1$

$$\Psi_{\beta,n}^p = \hat{\phi}'_{\beta,n} \cos\left(\frac{2np\pi}{N}\right) - \hat{\phi}''_{\beta,n} \sin\left(\frac{2np\pi}{N}\right). \quad (5)$$

where n is the circumferential wave number and β is the mode family.

However, by the fact each sector type mode is computed independently to the others, a phase shift can appear between cyclic modes of a modified blade computed on a sector p and the cyclic modes of the nominal blade, computed on the same sector. In fact, in tuned conditions, the location of the twin orthogonal modes on the bladed disk is indeterminate as shown on Fig. 1. On this figure, the two sub-figures on left represent the twin orthogonal modes, for the first computation. To address this

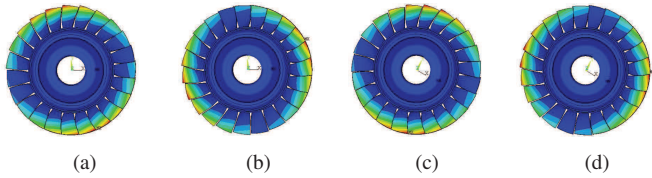


Figure 1. Geometries of twin modes with one nodal diameter obtained by two independent computations : first computation ((a),(b)) and second computation ((c),(d)).

problem, we introduce a modal scale factor MSF to make sure that cyclic modes of different sector kinds computed separately are taken in the same phase reference system. This modal scale factor is a complex number defined by

$$MSF(x,y) = \frac{\{x\}^T \{\bar{y}\}}{\{x\}^T \{\bar{x}\}}, \quad \text{where } x \text{ and } y \text{ are complex vectors.} \quad (6)$$

The argument of this modal scale factor represents the phase shift between the vectors x and y . By applying this scaling factor to the complex cyclic mode $\hat{\phi}_{\beta,n}^{ini}$ associated to the circumferential wave number n of one type of sector, we obtain the new modes $\hat{\phi}_{\beta,n}$ expressed in the phase reference system of the nominal blade

$$\hat{\phi}_{\beta,n} = \frac{MSF(\hat{\phi}_{\beta,n}^{nom}, \hat{\phi}_{\beta,n}^{ini})}{|MSF(\hat{\phi}_{\beta,n}^{nom}, \hat{\phi}_{\beta,n}^{ini})|} \hat{\phi}_{\beta,n}^{ini}, \quad (7)$$

where $\hat{\phi}_{\beta,n}^{nom}$ is the corresponding cyclic mode computed on the nominal sector.

In fact, we can verify in (8) that the new mode $\hat{\phi}_{\beta,n}$ is in phase with the nominal mode because its MSF referred to the nominal mode is real, implying that its argument is null.

$$MSF(\hat{\phi}_{\beta,n}^{nom}, \hat{\phi}_{\beta,n}) = \frac{\{\hat{\phi}_{\beta,n}^{nom}\}^T \{\overline{\hat{\phi}_{\beta,n}}\}}{\{\hat{\phi}_{\beta,n}^{nom}\}^T \{\overline{\hat{\phi}_{\beta,n}^{nom}}\}} = |MSF(\hat{\phi}_{\beta,n}^{nom}, \hat{\phi}_{\beta,n}^{ini})| \in \mathbb{R}, \quad (8)$$

where $|z|$ represents the modulus of complex z .

Then, after correcting the mode shapes obtained by two independent computations with their modal scale factor, Fig. 1 becomes Fig. 2, which exhibits phased mode shapes.

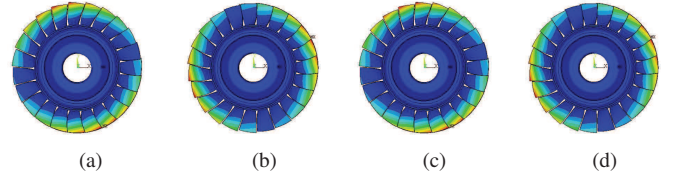


Figure 2. Geometries of twin modes with one nodal diameter obtained by two independent computations after correction using MSF: first computation ((a),(b)) and second computation ((c),(d)).

Generalized dynamic equation of the mistuned system: Let us introduce generalized coordinates representing the contribution of selected modes on the displacement field. Then, the displacement field can be written

$$\underline{u}(\omega) = [\Psi] \underline{q}(\omega), \quad (9)$$

where $\underline{q} = [q_0, \dots, q_{N-1}]^T$ is the complex-valued generalized coordinates vector associated to the system.

Thus, the generalized problem in global coordinates system becomes

$$[\underline{E}_{red}(\omega)] \underline{q}(\omega) = [\Psi]^T \underline{f}_{exc}(\omega) + [\Psi]^T \underline{f}_{aero}(\omega, [\Psi] \underline{q}(\omega)), \quad (10)$$

where the reduced dynamic (α^* , α^*) operator is a bloc diagonal matrix, because of the assumption of blade geometric detuning, defined by

$$[\underline{E}_{red}(\omega)] = [\Psi]^T [\underline{E}(\omega)] [\Psi], \quad (11)$$

$$[\underline{E}_{red}(\omega)]_{\beta,\alpha} = \sum_{p=0}^{N-1} \left(\Psi_{\beta}^{\Omega_p} \right)^T [\underline{E}(\omega)]^{pp} \left(\Psi_{\alpha}^{\Omega_p} \right), \quad (12)$$

and the generalized forces are defined by

$$\begin{aligned} \underline{g}_{exc}(\omega) &= [\Psi]^T \underline{f}_{exc}(\omega), \\ \underline{g}_{aero}(\omega, \underline{q}(\omega)) &= [\Psi]^T \underline{f}_{aero}(\omega, [\Psi] \underline{q}(\omega)), \end{aligned} \quad (13)$$

Clearly, the projection basis is constructed with respect to the distribution of the different sector's types and by keeping orthogonality properties between modes. Note that the reduced dynamic operator exhibits off diagonal. This implies that the detuning couples tuned cyclic modes with different number of nodal diameters.

Aerodynamic generalized forces can be express using a complex-valued aeroelastic matrix as:

$$\underline{g}_{aero}(\omega, [\Psi] \underline{q}(\omega)) = -[\underline{A}_{red}(\omega)] \underline{q}(\omega), \quad (14)$$

The real part of this aeroelastic matrix can be considered as a stiffness matrix and the imaginary part as a damping matrix. Then this matrix can be written

$$[\underline{A}_{red}(\omega)] = [\underline{A}_{red}^R(\omega)] + i[\underline{A}_{red}^I(\omega)], \quad i^2 = -1, \quad (15)$$

and the complete dynamic equation in generalized coordinates system yields

$$\begin{aligned} \{-\omega^2 [\underline{M}_{red}] + i\omega([\underline{D}_{red}] + [\underline{A}_{red}^I(\omega)]) + [\underline{K}_{red}] + [\underline{A}_{red}^R(\omega)]\} \underline{q}(\omega) \\ = \underline{g}_{exc}(\omega), \end{aligned} \quad (16)$$

Displacement field at coupling sector interfaces:

To solve the dynamic equation of motion of the detuned bladed disk, by using a projection basis made of different sector types cyclic modes, we must insure an admissible displacement field on the coupling sector interfaces. This admissibility is defined by two conditions on interfaces: a compatibility of meshes which is naturally insured because geometric modifications are only done on blades, and the displacement field continuity between two adjacent sectors which can be insured by linear constraints on the interface. These constraints can be introduced by using a Lagrange multiplier field (see [14]) or by expressing constrained generalized coordinates as a function of non constrained ones. The latter formulation is made here. Let us consider two sectors Ω^p and Ω^{p+1} , with $p \in [0, N-1]$, interacting through a common boundary Γ^p . The linear coupling condition on Γ^i can be written

$$\underline{u}^p = \underline{u}^{p+1} \quad \text{on} \quad \Gamma^p. \quad (17)$$

Then, on the entire structure, the physical displacement field \underline{u}_c can be written as a function of the free (non-constrained) displacement field \underline{u} by

$$\underline{u}_c = [\underline{B}] \underline{u}, \quad (18)$$

where $[\underline{B}]$ is an (n_{dof}, n_{dof}) integer continuity matrix in physical coordinates system, where n_{dof} is the sector degrees-of-freedom number. Thus, with generalized coordinates, we have

$$\underline{q}_c = [\underline{B}_{red}] \underline{q}, \quad [\underline{B}_{red}] = ([\Psi]^T [\Psi])^{-1} [\Psi] [\underline{B}] [\Psi], \quad (19)$$

where $[\underline{B}_{red}]$ is a $(\alpha^* \times \alpha^*)$ real continuity matrix in generalized coordinates system.

Thus, the problem, formulated on constrained-generalized coordinates system can be written

$$[\underline{E}_{red}] \underline{q}_c = \underline{g}_c, \quad (20)$$

Consequently, the problem, formulated on free-generalized coordinates system and including linear constraints that make the displacement field admissible over the entire structure is such that

$$[\underline{B}_{red}]^T [\underline{E}_{red}] [\underline{B}_{red}] \underline{q} = [\underline{B}_{red}]^T \underline{g}. \quad (21)$$

Note that while solving a reduced size problem, α^* is small and the $(\alpha^* \times \alpha^*)$ matrix $[\Psi]^T [\Psi]$ can easily be inverted.

VALIDATION OF THE REDUCTION METHOD

The realistic test case considered here is an industrial bladed disk with 23 blades. The commercial software used to compute the cyclic modes and mass and stiffness matrices for the reduced-order model inputs, and the forced response and resonant frequencies of the 360-deg full-rotor model is ANSYS.

Fig. 3 displays the eigenfrequencies of the generalized eigenproblem associated with the tuned bladed disk in function of the circumferential wave number.

To validate our method, we are going to approximate the 76 first modes of the mistuned bladed disk and to compute the forced response under 2 engine order excitation numbers. Note that the 100 first natural frequencies of the tuned bladed disk are above 5000Hz.

For the detuned system, two other kinds of blades are created from the nominal one by shape modification of the blade upper part: a blade with increased thickness called "heavy blade" and a blade with decreased thickness called "light blade" (see Fig. 4).

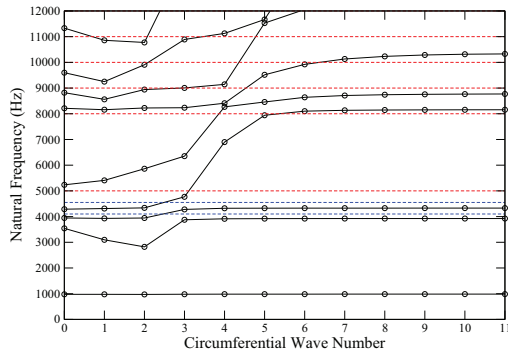


Figure 3. Natural frequencies versus circumferential wave numbers of the tuned bladed disk.

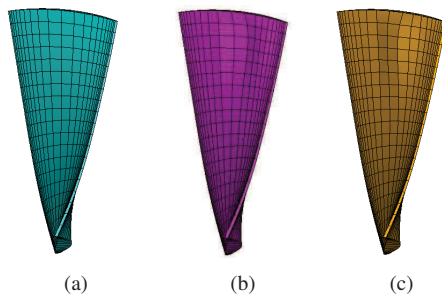


Figure 4. Finite element models of blades: a reference blade (a), a light blade (b) and a heavy blade (c).

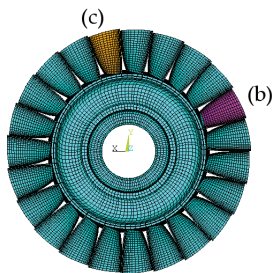


Figure 5. Complete intentionally detuned bladed disk with arbitrary geometric modification of two blades.

The bladed disk is detuned by modifying arbitrarily two of is blades to make them have the shapes shown on Fig. 4. The test case we study is shown on Fig. 5.

Fig. 6 and Fig. 7 display the 76 first eigenfrequencies of the generalized eigenproblem associated with the mistuned bladed disk and the corresponding mistuned frequencies errors. These eigenfrequencies are those of the tuned bladed disk under

5000Hz. Different analysis are carried out by taking different sizes of projection basis to obtain different reduced-order models (ROM): ROM-76-dof, ROM-133-dof, ROM-144-dof, ROM-160-dof, ROM-177-dof, obtained with tuned modes under 5000Hz, 8000Hz, 9000Hz, 10000Hz, 11000Hz, 12000Hz.

In this test, the natural frequency errors obtained for all approximated mistuned modes are below 0.4%, which demonstrates a sufficient accuracy in capturing the resonances of the detuned bladed disk.

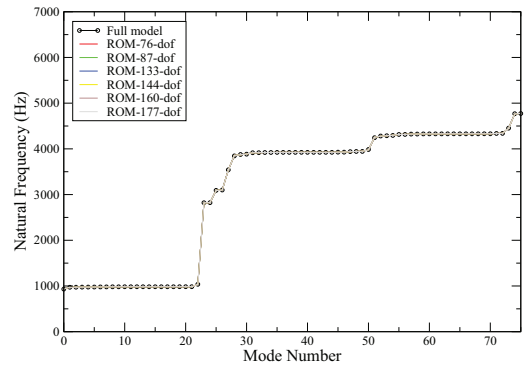


Figure 6. Comparison of the 76 first mistuned natural frequencies between the full model and several ROM sizes.

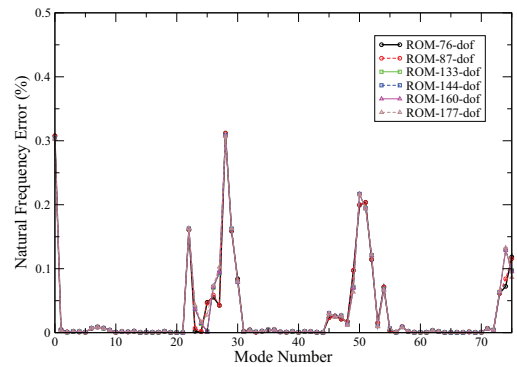


Figure 7. Comparison of the 76 first mistuned natural frequencies errors between the full model and several ROM sizes.

Note that the maximum error levels are obtained for resonances in which the vibrational energy is mainly located on the disk, and that the resonances for which the vibrational energy is mainly located on the blades are precisely obtained, with an error level below 0.01%. The latter case resonances can be easily identified as the clustered modes near frequencies 1000Hz, 4000Hz

and 4400Hz on Fig. 6. Note also the ROM-76-dof accuracy in predicting the 76 first resonances of the mistuned bladed disk, which shows a quite compact model.

For the forced response consideration, all blades responses under engine orders excitation 5 and 9 are computed in the frequency band 4150-4550 Hz and displayed on Fig. 8 and Fig. 9.

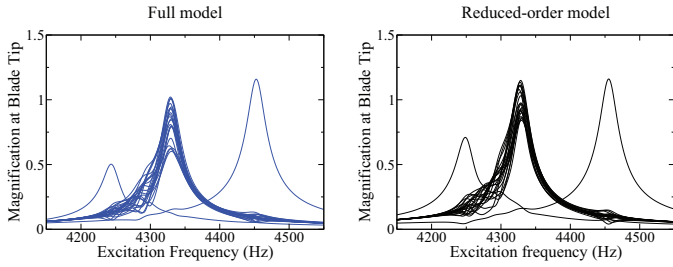


Figure 8. Forced response of the 23 blades to an engine order excitation 5 in the frequency band 4150-4550 Hz: Full model (left) and ROM (right).

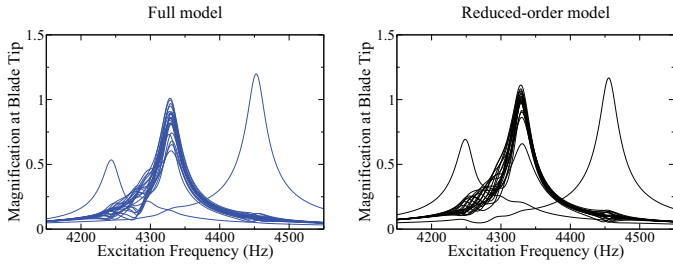


Figure 9. Forced response of the 23 blades to an engine order excitation 9 in the frequency band 4150-4550 Hz: Full model (left) and ROM (right).

On these figures, both the 360-deg full-rotor model and the ROM exhibit a clustered response of 21 blades and 2 isolated responses which are the modified blades responses. Moreover, the dynamic behavior of the full bladed disk model is quite similar to the ROM one.

The results obtained above demonstrate a sufficient accuracy of the proposed ROM in capturing the detuned bladed disk, in both free and forced response configurations.

NONPARAMETRIC MODEL OF RANDOM UNCERTAINTIES FOR BLADE MISTUNING

The purpose here is to model the random uncertainties due to mistuning. Mistuning is assumed to be statistically independent from blade to blade. To take into account model and data

uncertainties, a nonparametric probability model of random uncertainties is used. The main results concerning this nonparametric probability model of random uncertainties construction in structural dynamics can be found in [15]. This probabilistic approach requires the construction of a mean reduced matrix model for each uncertain sector. The probability model has to be consistent with the mechanical problem. Thus, it has to satisfy the following constraints which constitute the only available information:

- C1: the mean reduced matrix is equal to the mean value of the random reduced matrix;
- C2: the signature of the random reduced matrix is respected: it means that the random reduced matrix has to be positive definite if its corresponding mean reduced matrix is positive definite;
- C3: the second-order moment of the physical random response of the bladed disk has to exist, for getting a second-order displacement field.

The probability model is then derived from these three constraints by using the entropy maximization principle.

Random Reduced Matrix Model for the Bladed-Disk

using the methodology derived from [3, 15], the nonparametric probabilistic approach consists in modeling the reduced dynamic stiffness matrix for sector p as the random matrix

$$[\mathbf{E}_{red}(\omega)^p] = -\omega^2 [\mathbf{M}_{red}^p] + i\omega [\mathbf{D}_{red}^p] + [\mathbf{K}_{red}^p], \quad (22)$$

in which $[\mathbf{M}_{red}^p]$, $[\mathbf{D}_{red}^p]$ and $[\mathbf{K}_{red}^p]$ are independent random matrices corresponding to the random reduced mass, damping, and stiffness matrices of sector p , and modeling the complex aeroelastic matrix as the random matrix $[\mathbf{A}_{red}(\omega)^p]$.

Then, constraints C1 can be written on random matrices

$$\begin{aligned} \mathcal{E}\{[\mathbf{M}_{red}^p]\} &= [\underline{\mathbf{M}}_{red}^p], & \mathcal{E}\{[\mathbf{D}_{red}^p]\} &= [\underline{\mathbf{D}}_{red}^p], \\ \mathcal{E}\{[\mathbf{K}_{red}^p]\} &= [\underline{\mathbf{K}}_{red}^p], & \mathcal{E}\{[\mathbf{A}_{red}^p]\} &= [\underline{\mathbf{A}}_{red}^p], \end{aligned} \quad (23)$$

where $\mathcal{E}\{\cdot\}$ is the mathematical expectation.

To do so, we need to normalize the mass, damping, stiffness and aeroelastic random matrices as well as the mean value of each normalized random matrix is the unity matrix. Such a construction requires the factorization of the mean reduced matrices.

The mean reduced mass, damping and stiffness matrices are real positive definite matrices. So, their Choleski factorization yields

$$[\underline{\mathbf{M}}_{red}^p] = [\underline{\mathbf{L}}_M^p]^T [\underline{\mathbf{L}}_M^p], \quad [\underline{\mathbf{D}}_{red}^p] = [\underline{\mathbf{L}}_D^p]^T [\underline{\mathbf{L}}_D^p], \quad [\underline{\mathbf{K}}_{red}^p] = [\underline{\mathbf{L}}_K^p]^T [\underline{\mathbf{L}}_K^p], \quad (24)$$

Then, the real random matrices can be written as

$$\begin{aligned} [\mathbf{M}_{red}^p] &= [\underline{L}_M^p]^T [\mathbf{G}_M^p] [\underline{L}_M^p], & [\mathbf{D}_{red}^p] &= [\underline{L}_D^p]^T [\mathbf{G}_D^p] [\underline{L}_D^p], \\ [\mathbf{K}_{red}^p] &= [\underline{L}_K^p]^T [\mathbf{G}_K^p] [\underline{L}_K^p], \end{aligned} \quad (25)$$

where $[\mathbf{G}_M^p]$, $[\mathbf{G}_D^p]$ and $[\mathbf{G}_K^p]$ are real normalized random matrices whose mean value is the unity matrix.

For the complex aeroelastic matrix, we use a singular value decomposition in the factorization process defined in [16]. By this way, the complex matrix $[\underline{A}_{red}]$ can be written

$$[\underline{A}_{red}(\omega)] = [\underline{U}(\omega)] [\underline{T}(\omega)], \quad (26)$$

where $[\underline{U}(\omega)]$ is a complex unitary matrix and $[\underline{T}(\omega)]$ is a complex positive definite matrix admitting a Choleski factorization.

Then, we propose a random modeling of the aeroelastic matrix

$$[\underline{A}_{red}(\omega)] = [\underline{U}(\omega)] [\underline{L}_T(\omega)]^T [\mathbf{G}_A] [\underline{L}_T(\omega)], \quad (27)$$

where $[\mathbf{G}_A]$ is a real normalized random matrix whose mean value is the unity matrix.

Constraints C2 and C3 mean that the normalized random matrices $[\mathbf{G}_M^p]$, $[\mathbf{G}_D^p]$, $[\mathbf{G}_K^p]$ and $[\mathbf{G}_A]$ are real positive definite matrices verifying

$$\begin{aligned} \mathcal{E}\{\|[\mathbf{G}_M^p]^{-1}\|_F^2\} &< +\infty, & \mathcal{E}\{\|[\mathbf{G}_D^p]^{-1}\|_F^2\} &< +\infty, \\ \mathcal{E}\{\|[\mathbf{G}_K^p]^{-1}\|_F^2\} &< +\infty, & \mathcal{E}\{\|[\mathbf{G}_A]^{-1}\|_F^2\} &< +\infty, \end{aligned} \quad (28)$$

where $\|[\cdot]\|_F = (\text{tr}([\cdot][\cdot]^T))^{\frac{1}{2}}$. The dispersion level of these four normalized random matrices can be controlled by the positive real parameters δ_M^p , δ_D^p , δ_K^p and δ_A defined by

$$\delta_F = \left\{ \frac{\mathcal{E}\{\|[\mathbf{G}_F] - [\underline{G}_F]\|_F^2\}}{[\underline{G}_F]} \right\}^{\frac{1}{2}} \quad \text{with } F = \{\mathbf{M}, \mathbf{D}, \mathbf{K}, \mathbf{A}\}. \quad (29)$$

From equations (25) and (27), it can be deduced that these parameters allow the dispersion level of random matrices $[\mathbf{M}_{red}^p]$, $[\mathbf{D}_{red}^p]$, $[\mathbf{K}_{red}^p]$ and $[\underline{A}_{red}]$ to be controlled.

Probability Model of the Random Matrices

Using the entropy maximization principle with available information defined by constraints C1, C2 and C3 related to the normalized random matrices, it can be proved, [15], that the algebraic representation of matrix $[\mathbf{G}]$ allows a procedure for the

Monte Carlo numerical simulation of random matrix $[\mathbf{G}]$ to be defined. According to [15] in which all the details concerning the construction of the probability model of the normalized random matrix $[\mathbf{G}]$ can be found, the random matrix $[\mathbf{G}]$ can be written

$$[\mathbf{G}] = [L_G]^T [L_G], \quad (30)$$

in which $[L_G]$ is an $n \times n$ real upper triangular random matrix such that

- random variables $\{[L_G]_{jj'}, j \leq j'\}$ are independent;
- for $j < j'$, real-valued random variable $[L_G]_{jj'}$ can be written as

$$[L_G]_{jj'} = \delta(n+1)^{-1/2} U_{jj'}, \quad (31)$$

in which $U_{jj'}$ is a real-valued Gaussian random variable with zero mean value and variance equal to 1;

- for $j = j'$, positive-valued random variable $[L_G]_{jj}$ can be written as

$$[L_G]_{jj} = \delta(n+1)^{-1/2} \sqrt{2V_j}, \quad (32)$$

in which V_j is a positive-valued gamma random variable whose probability density function $p_{V_j}(v)$ with respect to dv is written as

$$p_{V_j}(v) = \mathbb{1}_{\mathbb{R}^+}(v) \frac{1}{\Gamma(\alpha_{n,j})} v^{(\alpha_{n,j})-1} e^{-v}, \quad \alpha_{n,j} = \frac{n+1}{2\delta^2} + \frac{1-j}{2}. \quad (33)$$

NUMERICAL EXAMPLE FOR AN INDUSTRIAL BLADED DISK

The bladed disk considered is the same blade disk used to validate the reduced-order model. This bladed disk is considered under rotation. Mistuning is modeled here using the non parametric probabilistic method and detuning is introduced by performing a shape modification of some blades and distributing these blades so that they create alternate mistuning.

For the forced response considerations, a conventional 9 engine order excitation is considered in the analysis over an excitation frequency range $\mathbb{B} = [4400, 4750]$ Hz.

Forced response amplitudes of the mistuned system are normalized with respect to the maximum amplitudes of the equivalent tuned bladed disk under the same excitation conditions. The structural damping loss factor is set to 0.003. For the reduced order model, the projection basis is constituted of modes belonging to the frequency band $[0, 5000]$ Hz.

Detuning method

Different types of intentional mistuning patterns have been adopted in the past, such as alternate mistuning, by alternating high and low frequency blades [17], periodic mistuning [18, 19], harmonic mistuning [6–8, 20], and linear mistuning [21]. The purpose here is not to find the best intentional mistuning pattern but to analyze the the forced response sensitivity to mistuning, of a detuned system with a fixed chosen pattern. For the sake of simplicity, we only consider two kinds of blades : a reference blade and a lower frequency blade. So the fixed pattern chosen here is an alternate mistuning pattern which consist on alternating 6 reference blades and 6 lower frequency blades.

To get the lower frequency blades, blade shapes are modified by retrieving locally 20% of the blade thickness on the upper part of the blade and adding locally 20% of the blade thickness on the lower part. This can be called a 20% modification. We present on Fig. 10, a 80% modification to highlight the geometric modification performed.

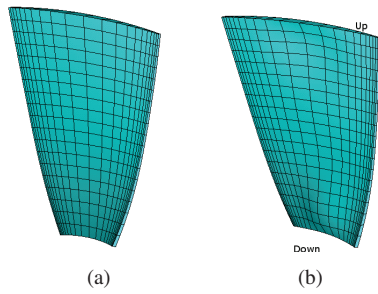


Figure 10. Reference blade shape (a) and modified blade shape (b).

To estimate the level of perturbation induced by this modification on aerodynamic characteristics, the Mach field (see Fig. 11) has been displayed on the different kinds of blades in cyclic symmetry configuration. Thus, we can see that the air flow has not greatly been perturbed, but little differences may appear on the damping characteristics of the two kinds of blade. These differences can be taken into account by the stochastic process, but to do so, we need a method of estimating the aeroelastic dispersion parameter between the two configurations like the one developed in [22]. For the sake of simplicity, this will not be treated here, and an aeroelastic null dispersion parameter is considered here for the test.

Random magnification factor

Mistuning is expressed in terms of dispersion level of the stiffness matrix. In fact, in [22], by solving the inverse problem of specifying the blade manufacturing tolerances, it was found

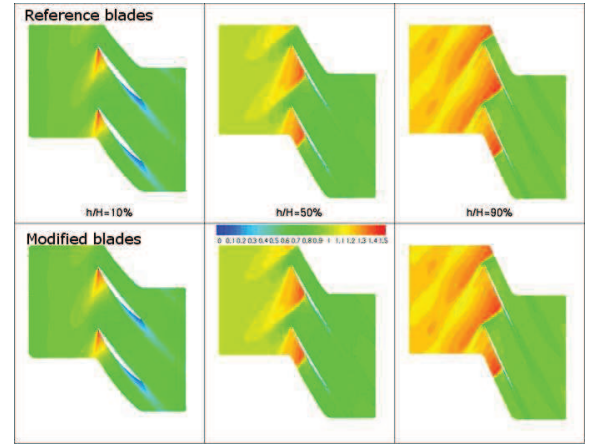


Figure 11. Comparison of the Mach field on reference and modified blades.

that the dispersion level of the mass matrix induced by manufacturing tolerances is about 1000 times less than the stiffness matrix one.

The observation considered here to control the forced response is the random dynamic magnification factor $\{\mathbf{B}(\omega), \omega \in \mathbb{B}\}$ which is such that

$$\mathbf{B}(\omega) = \sup_{p \in \{0, \dots, N-1\}} \mathbf{B}^p(\omega), \quad \mathbf{B}^p(\omega) = \frac{|\mathbf{u}^p(\omega)|}{\underline{u}^p},$$

$$\underline{u}^p = \sup_{\omega \in \mathbb{B}(\omega)} |\mathbf{u}^p(\omega)|, \quad B_\infty = \sup_{\omega \in \mathbb{B}(\omega)} \mathbf{B}(\omega), \quad (34)$$

in which for blade p , $\mathbf{u}^p(\omega)$ is the random variable of the physical displacement of a tip node of the vibrating blade p , $\underline{u}^p(\omega)$ is the mean random variable of the physical displacement of a tip node of the vibrating blade p and $(\sup_n M)$ is the maximum value of M over the domain defined by n . B_∞ is the random dynamic magnification factor over the frequency band \mathbb{B} .

The realizations of random observation B_∞ are deduced from the Monte Carlo numerical simulations and mathematical statistics are used for estimating probability.

A convergence analysis has been carried out for the magnification factor. Since the second-order mean convergence yields the convergence in law, the convergence analysis can be limited to the second-order convergence of random magnification factor and damping coefficient.

A 1000 Monte Carlo simulation has been performed for each value of δ_K and Fig. 12 shows that convergence is already reached for 500 simulations.

Fig. 13 shows a well known behavior of small mistuned bladed disks: the forced response increases for low rates of mis-

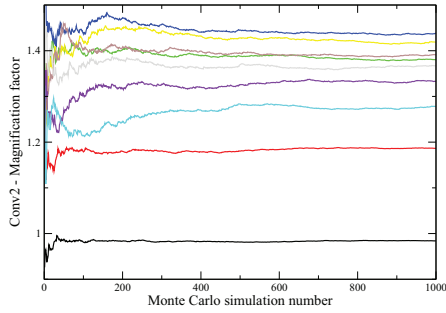


Figure 12. Second-order mean convergence of B_∞ with mistuning: (curves, from the lower to the upper correspond respectively at Monte Carlo simulation number 1000 to $\delta_{\mathbf{K}}=0.005$, $\delta_{\mathbf{K}}=0.01$, $\delta_{\mathbf{K}}=0.1$, $\delta_{\mathbf{K}}=0.02$, $\delta_{\mathbf{K}}=0.07$, $\delta_{\mathbf{K}}=0.06$, $\delta_{\mathbf{K}}=0.05$, $\delta_{\mathbf{K}}=0.04$ and $\delta_{\mathbf{K}}=0.03$.)

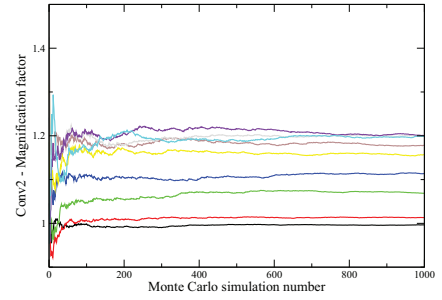


Figure 14. Second-order mean convergence of B_∞ with mistuning and detuning: (curves, from the lower to the upper correspond respectively at Monte Carlo simulation number 600 to $\delta_{\mathbf{K}}=0.005$, $\delta_{\mathbf{K}}=0.01$, $\delta_{\mathbf{K}}=0.01$, $\delta_{\mathbf{K}}=0.03$, $\delta_{\mathbf{K}}=0.04$, $\delta_{\mathbf{K}}=0.05$, $\delta_{\mathbf{K}}=0.1$, $\delta_{\mathbf{K}}=0.06$ and $\delta_{\mathbf{K}}=0.07$.)

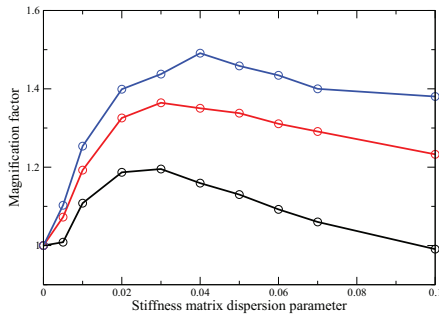


Figure 13. Influence of the mistuning rate: graph such that $P(B_\infty \leq B_p) = p$ (the lower, middle and upper curves correspond respectively to a probability level $p=0.50$, $p=0.95$ and $p=0.99$.)

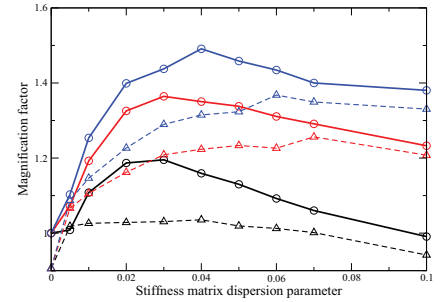


Figure 15. Influence of the mistuning rate: graph such that $P(B_\infty \leq B_p) = p$ (the continuous curves with circles (and non continuous curves with triangles) are related to the tuned (and detuned) system. The lower, middle and upper curves correspond respectively to a probability level $p=0.50$, $p=0.95$ and $p=0.99$.)

tuning, reaches a maximum value and decreases slightly while the level of mistuning still increases.

Sensitivity analysis of mistuning for a given detuning

The purpose here is to reduce the bladed disk sensitivity to mistuning by reducing the forced response magnification induced. Thus, we are interested in relatively small mistuning.

A 1000 Monte Carlo simulation has also been performed here for each value of $\delta_{\mathbf{K}}$ and Fig. 14 shows that convergence is reached for this number simulation, although the bladed disk is detuned. The detuning performed here is very effective for low mistuning levels as shown on Fig. 15. While the reference magnification factor has a bell behavior, the detuned system magnification factor has a continuous lightly increasing curve which still remain under reference curve for the three probability levels observed. Moreover, at high mistuning levels, the detuned magnification factor curves tends to the reference one, showing that at high mistuning levels, the disorder degree is so high that the detuning performed is cover by the mistuning.

CONCLUSION

A way to perform robust design of bladed disks in forced response considerations by geometric modification of blades is investigated. In this context, a new reduction method using the cyclic modes of the different kinds of sectors is developed. Detuning is performed here by modifying blade shapes without perturbing a lot the aerodynamic characteristics. To take into account mistuning, a non parametric probabilistic model taking into account model and parameters uncertainties is built on the mean reduced model. An example of reducing a bladed disk sensitivity to mistuning is finally presented. This analysis shows that although the detuning pattern is not optimized, the geometric modifications of blades can reduce blade sensitivity to mistuning. Then, by combining a blade geometric modification with a detuning pattern optimization like the one proposed in [5, 23], an optimal robust design model minimizing the forced response while keeping stability could be obtained. This is the purpose of our future works.

ACKNOWLEDGMENT

Turbomeca Company is gratefully acknowledged for the permission to publish this work. The authors also wish to thank reviewers for their comments.

REFERENCES

- [1] Whitehead, D., 1966. "Effects of Mistuning on the Vibration of Turbomachine Blades Induced by Wakes". *Journal of Mechanical Engineering Science*, **8**(1), pp. 15–21.
- [2] Dye, R., and Henry, T., 1969. "Vibration Amplitudes of Compressor Blades Resulting from Scatter in Blade Natural Frequencies". *ASME Journal of Engineering for Power*, **91**(3), pp. 182–187.
- [3] Capiez-Lernout, E., and Soize, C., 2004. "Nonparametric Modeling of Random Uncertainties for Dynamic Response of Mistuned Bladed-disks". *ASME Journal of Engineering for Gas Turbines and Power*, **126**(3), pp. 610–618.
- [4] Ewins, D., 1969. "The Effects of Detuning upon the Forced Vibrations of Bladed Disks". *Journal of Sound and Vibration*, **9**(1), pp. 65–69.
- [5] Choi, B.-K., Lentz, J., Rivas-Guerra, A., and Mignolet, M., 2003. "Optimization of Intentional Mistuning Patterns for the Reduction of the Forced Response Effects of Unintentional Mistuning: Formulation and Assessment". *ASME Journal of Engineering for Gas Turbines and Power*, **125**, pp. 131–140.
- [6] Castanier, M., Ottarson, G., and Pierre, C., 1997. "Reduced Order Modeling Technique for Mistuned Bladed Disks". *ASME Journal of Vibration and Acoustics*, **119**(3), pp. 439–447.
- [7] Castanier, M., and Pierre, C., 2002. "Using Intentional Mistuning in the Design of Turbomachinery rotors". *AIAA Journal*, **40**(10), pp. 2077–2086.
- [8] Mignolet, M., Hu, W., and Jadic, I., 2000. "On the Forced Response of Harmonically and Partially Mistuned Bladed Disks. part 1: Harmonic Mistuning, part 2: Partial Mistuning and Applications". *International Journal of Rotating Machinery*, **6**(1), pp. 29–56.
- [9] Yang, M.-T., and Griffin, J., 2001. "A Reduced-Order Model of Mistuning using a Subset of Nominal System Modes". *ASME Journal of Engineering for Gas Turbines and Power*, **123**(3), pp. 893–900.
- [10] Feiner, D., and Griffin, J., 2002. "A fundamental model of mistuning for a single family of modes". *Journal of Turbomachinery*, **124**, pp. 597–605.
- [11] Feiner, D., and Griffin, J., 2002. "Mistuning identification of bladed disks using fundamental mistuning model. part 1: Theory, part 2: Application". *Journal of Turbomachinery*, **126**, pp. 150–165.
- [12] Lim, S.-H., Castanier, M., and Pierre, C., 2004. "Vibration modeling of bladed disks subject to geometric mistuning and design changes". In Proceedings of the 45-th AIAA/ASME/ASCE/AHS/ASC Structures, Structural Dynamics and Material Conference, paper 2004-1686, Palm Springs, California, USA.
- [13] Mbaye, M., Soize, C., Ousty, J.-P., and Capiez-Lernout, E., 2009. "A reduced-order model of mistuned cyclic dynamical systems with finite geometric perturbations using a basis of cyclic modes". In Proceedings of the XIII International Symposium on Dynamic Problems of Mechanics, paper DIN09-0133, Angra dos Reis, Rio de Janeiro, Brazil.
- [14] Ohayon, R., Sampaio, R., and Soize, C., 1997. "Dynamic Substructuring of Damped Structures using the Singular Value Decomposition". *ASME Journal of Applied Mechanics*, **64**(2), pp. 292–298.
- [15] Soize, C., 2001. "Maximum Entropy Approach for Modeling Random Uncertainties in Transient Elastodynamics". *Journal of the Acoustical Society of America*, **109**(5), pp. 1979–1996.
- [16] Soize, C., 2005. "Random Matrix Theory for Modeling Uncertainties in Computational Mechanics". *Computer Methods in Applied Mechanics and Engineering*, **194**, pp. 1333–1366.
- [17] Griffin, J. H., and Hoosac, T. M., 1984. "Model development and statistical investigation of turbine blade mistuning". *ASME Journal of Vibration, Acoustics, Stress, and Reliability in Design*, **106**, pp. 204–210.
- [18] Imregun, M., and Ewins, D. J., 1984. "Aeroelastic vibration analysis of tuned and mistuned bladed systems". In Proceedings of the Second Symposium on Unsteady Aerodynamics of Turbomachines and Propellers, Cambridge, UK.
- [19] Rzadkowski, R., 1993. "The general model of free vibrations of mistuned bladed discs, part 1: Theory, part 2: Numerical results". *Journal of Sound and Vibration*, **173**(3), pp. 377–393.
- [20] Kenyon, J. A., and Griffin, J. H., 2001. "Forced response of turbine engine bladed disks and sensitivity to harmonic mistuning". In Proceedings of the ASME TURBO EXPO 2001, 2001-GT-0274.
- [21] Jones, W. J., and Cross, C. J., 2002. "Reducing mistuned bladed disk forced response below tuned resonant amplitudes". In Seventh National Turbine Engine High Cycle Fatigue Conference, Palm Beach, FL, USA.
- [22] Capiez-Lernout, E., Soize, C., Lombard, J.-P., Dupont, C., and Seinturier, E., 2005. "Blade Manufacturing Tolerances Definition for a Mistuned Industrial Bladed Disk". *ASME Journal of Engineering for Gas Turbines and Power*, **127**(2), pp. 621–628.
- [23] Han, Y., and Mignolet, M. P., 2008. "Optimization of intentional mistuning patterns for the mitigation of the effects of random mistuning". In Proceedings of the ASME TURBO EXPO 2008, GT-2008-51439.